© 2014. Published by The Company of Biologists Ltd | Development (2014) 141, 1961-1970 doi:10.1242/dev.106310

RESEARCH ARTICLE

Noonan and LEOPARD syndrome Shp2 variants induce heart displacement defects in zebrafish

Monica Bonetti[1], Jeroen Paardekooper Overman[1], Federico Tessadori[1], Emily Noël[1], Jeroen Bakkers[1] and Jeroen den Hertog[1,2,*]

ABSTRACT

Germline mutations in *PTPN11*, encoding Shp2, cause Noonan syndrome (NS) and LEOPARD syndrome (LS), two developmental disorders that are characterized by multiple overlapping symptoms. Interestingly, Shp2 catalytic activity is enhanced by NS mutations and reduced by LS mutations. Defective cardiac development is a prominent symptom of both NS and LS, but how the Shp2 variants affect cardiac development is unclear. Here, we have expressed the most common NS and LS Shp2-variants in zebrafish embryos to investigate their role in cardiac development *in vivo*. Heart function was impaired in embryos expressing NS and LS variants of Shp2. The cardiac anomalies first occurred during elongation of the heart tube and consisted of reduced cardiomyocyte migration, coupled with impaired leftward heart displacement. Expression of specific laterality markers was randomized in embryos expressing NS and LS variants of Shp2. Ciliogenesis and cilia function in Kupffer's vesicle was impaired, likely accounting for the left/right asymmetry defects. Mitogen-activated protein kinase (MAPK) signaling was activated to a similar extent in embryos expressing NS and LS Shp2 variants. Interestingly, inhibition of MAPK signaling prior to gastrulation rescued cilia length and heart laterality defects. These results suggest that NS and LS Shp2 variant-mediated hyperactivation of MAPK signaling leads to impaired cilia function in Kupffer's vesicle, causing left-right asymmetry defects and defective early cardiac development.

KEY WORDS: Noonan syndrome, LEOPARD syndrome, Shp2, MAPK, Zebrafish

INTRODUCTION

PTPN11 encodes Shp2 (Ptpn11 – Zebrafish Information Network), a ubiquitously expressed non-receptor protein-tyrosine phosphatase (PTP) with two Src homology 2 (SH2) domains (Freeman et al., 1992; Feng et al., 1993; Chan and Feng, 2007) that is involved in a variety of signal transduction processes, such as the Ras-Raf-MAP kinase (Tidyman and Rauen, 2009), Jak-Stat (Freeman et al., 1992; Neel et al., 2003) and phosphatidylinositol-3 kinase (PI-3K) pathways (Feng, 1999). Shp2 plays a crucial role in the transduction of the signal from receptor tyrosine kinases (RTKs), including the receptors of platelet-derived growth factor (Pdgfr) (Van Vactor et al., 1998), fibroblast growth factor (Fgfr) (Neel and Tonks, 1997) and the epidermal growth factor (Egfr) (Huyer and Alexander, 1999; Qu, 2000), as well as from cytokine receptors and integrins (Neel and Tonks, 1997; Huyer and Alexander, 1999).

Missense germline mutations in *PTPN11* are associated with Noonan syndrome (NS) (OMIM: 163950) and LEOPARD syndrome (LS) (OMIM: 151100), two autosomal dominant disorders. NS is a relatively common disorder that affects 1 in 1000-2000 live births. Individuals with NS are characterized by congenital heart defects, including atrial and ventricular septal defects, pulmonary stenosis and hypertrophic cardiomyopathy (HCM) (Tartaglia et al., 2001; Digilio et al., 2002). In addition, these individuals display short stature and facial abnormalities. LS is a more rare disorder (1:3500 live births) that shows a substantial overlap with the various symptoms of NS with two more clinical manifestations that are specific for LS: deafness and 'café au lait' spots on the skin (Mendez and Opitz, 1985; Legius et al., 2002). The congenital heart defects among individuals with *PTPN11* mutations differ between NS and LS, in that pulmonary stenosis is most common in NS, whereas HCM prevails in LS (Allanson and Roberts, 1993; Sarkozy et al., 2008).

Interestingly, the biochemical properties of NS-Shp2 and LS-Shp2 are distinct, in that NS mutations enhance catalytic activity and LS mutations strongly reduce PTP activity (Keilhack et al., 2005; Kontaridis et al., 2006). The crystal structure of Shp2 shows that, in the absence of a binding partner, the N-SH2 domain interacts with the PTP domain and blocks the catalytic site (Hof et al., 1998). NS mutations predominantly reside in the interface between the N-SH2 domain and the PTP domain, resulting in the disruption of the closed conformation and enhanced catalytic activity of NS-Shp2 (Keilhack et al., 2005; Nakamura et al., 2009). By contrast, most LS mutations reside close to the active site and result in strongly reduced, yet detectable, catalytic activity (Keilhack et al., 2005; Hanna et al., 2006; Yu et al., 2013). How two mutations with opposite effects on catalytic activity result in syndromes withsimilar clinical symptoms is a conundrum that still needs to be resolved.

NS-Shp2 causes upregulation of the MAPK pathway (Feng, 1999). Whereas several studies show that LS mutations downregulate the level of phosphorylated ERK (Kontaridis et al., 2006; Stewart et al., 2010), the role of LS-Shp2 mutation on the MAPK pathway is still controversial (Oishi et al., 2006, 2009; Edouard et al., 2010). Increased RAS/MAPK signaling is implicated in the gain-of-function phenotypes that are caused by expression of the LS *Drosophila* ortholog of *PTPN11*, *corkscrew* (*csw*) (Oishi et al., 2009), suggesting a mechanism by which NS and LS variants may result in similar phenotypes. However, NS and LS signaling are distinct, because it is well established that LS mutations, but not NS mutations (De Rocca Serra-Nedelec et al., 2012), enhance PI3K/AKT signaling in hearts of LS/+ knock-in mice (Kontaridis et al., 2006) as well as in fibroblasts isolated from individuals with LS (Edouard et al., 2010). The similarities in RAS/MAPK signaling of NS and LS variants may underlie the overlapping symptoms in NS and LS, whereas the

[1]Hubrecht Institute-KNAW and University Medical Center Utrecht, Utrecht 3584 CT, The Netherlands. [2]Institute of Biology, Leiden 2333 CC, The Netherlands.

*Author for correspondence (j.denhertog@hubrecht.eu)

Received 21 November 2013; Accepted 11 March 2014

Development (2014) 141, 1961-1970 doi:10.1242/dev.106310

differences in PI3K/Akt signaling may cause the differences in NS- and LS-induced developmental defects.

Shp2 knockout, knockdown and gain-of-function studies in a variety of organisms have begun to reveal the roles of Shp2 in embryonic development. *Shp2*-null mouse embryos die pre-implantation due to defective Erk activation and trophoblast stem cell death (Yang et al., 2006). Dominant-negative *Shp2* mutants disrupt gastrulation in *Xenopus* (Tang et al., 1995). Moreover, mouse models have been generated for the two most prevalent NS and LS mutations, Ptpn11-D61G/+ and Ptpn11-Y279C/+, respectively. These mice exhibit developmental defects, including reduced length, craniofacial abnormalities and congenital heart defects, reminiscent of the clinical characteristics of the human disorders (Araki et al., 2004; Marin et al., 2011). In particular, pulmonary stenosis and HCM are evident in the NS and LS mice, respectively. Shp2 is conserved in zebrafish and we previously generated the most common human NS and LS mutations in a cDNA encoding full-length zebrafish Shp2. Micro-injection of mRNA-encoding mutant Shp2 variants into zebrafish embryos at the one-cell stage induces gastrulation cell movement defects, as well as craniofacial and cardiac defects (Jopling et al., 2007). Furthermore, Stewart et al. used zebrafish embryos to show that the function of Shp2 in neural crest cells underlies LS pathogenesis (Stewart et al., 2010).

The role of NS and LS Shp2 variants in the development of cardiac defects is still unclear. Zebrafish has become a powerful model with which to study cardiac development in recent years (Bakkers, 2011; Lien et al., 2012). We set out to study early heart development in zebrafish embryos expressing NS and LS variants of Shp2, taking advantage of the transparency of zebrafish embryos, which facilitates time-lapse analysis of the onset and nature of the cardiac defects *in vivo*. Our analyses revealed impaired heart function and morphogenesis, which were highly similar in NS- and LS-Shp2-expressing embryos. Furthermore, the heart defects were accompanied by randomization of left-right asymmetry, which was probably due to impaired ciliogenesis and defective cilia function in Kupffer's vesicle that we observed in early embryos. Treatment with a MEK-inhibitor, CI-1040, prior to gastrulation rescued defective leftward heart displacement and the laterality defects in NS- and LS-Shp2-expressing embryos. Taken together, our results provide insight into the mechanism by which NS and LS Shp2 variants induced laterality defects through hyperactivation of MAPK signaling, resulting in cardiac defects during early development.

RESULTS

Expression of NS and LS Shp2 variants caused defects in cardiac function

To investigate the role of Shp2 variants in cardiac function, Shp2-D61G and Shp2-A462T mRNAs were injected at the one-cell stage. In order to monitor expression of mutant Shp2, we fused a green fluorescent protein (GFP)-peptide 2A sequence to the N terminus of Shp2, which is cleaved off auto-proteolytically (Kim et al., 2011) (supplementary material Fig. S1). Following expression of (mutant) Shp2, the developing heart was analyzed at 55 hpf by high-speed video recording. Kymographs of the atrium and ventricle were generated, allowing quantification of heart function, as described previously (Tessadori et al., 2012). Representative examples of kymographs of embryos expressing WT-Shp2 and Shp2-D61G are depicted in Fig. 1A-F. Quantification of the kymographs of Shp2-WT-, Shp2-D61G- and Shp2-A462T-injected embryos revealed significantly longer cardiac cycles in the Shp2 variant-expressing embryos, reflecting a reduced but regular heart rate (Fig. 1G). Other functional defects, such as an atrioventricular block or uncoupling of the two chambers, were not detected in Shp2-D61G- and Shp2-A462T-expressing embryos. These results illustrate functional cardiac defects, particularly a reduced heart rate, in embryos expressing NS and LS variants of Shp2.

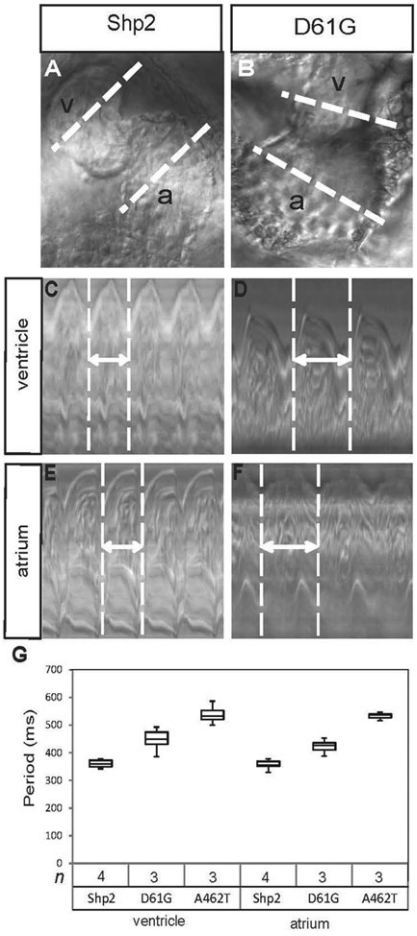

Fig. 1. Impaired cardiac function in embryos expressing Shp2-D61G and Shp2-A462T. (A,B) The hearts of WT-Shp2- (Shp2) and Shp2-D61G-expressing zebrafish embryos were imaged by high-speed video recording microscopy at 2 dpf. White dotted lines through the atrium (a) and the ventricle (v) are indicated. (C-F) Ventricular (C,D) and atrial (E,F) kymographs from 2 dpf embryonic hearts. Note the longer period of the Shp2-D61G-expressing heart, compared with the WT-Shp2-expressing heart (double-headed arrow and white dotted vertical lines). (G) Quantitative analysis of the heart period in the ventricle or atrium of WT-Shp2, Shp2-D61G and Shp2-A462T expressing embryos (*n* indicates number). Whisker plots are depicted.

Impaired heart asymmetry in embryos expressing NS and LS Shp2 variants

To further characterize the cardiac phenotype in response to expressing of NS and LS variants of Shp2, we first examined the overall morphology and regionalization of the heart at 55 hpf by *in situ* hybridization (ISH), using a panel of cardiac markers. At this stage, the heart chambers are completely formed in wild-type embryos and the heart undergoes looping morphogenesis. Analysis of heart shape using a *myl7*-specific probe (formerly known as *cmlc2*) revealed that the hearts of Shp2-D61G- and Shp2-A462T-expressing embryos exhibited either inverted looping (14% and 11%, respectively) or non-looped heart (39% and 25%, respectively) in contrast to non-injected

Development (2014) 141, 1961-1970 doi:10.1242/dev.106310

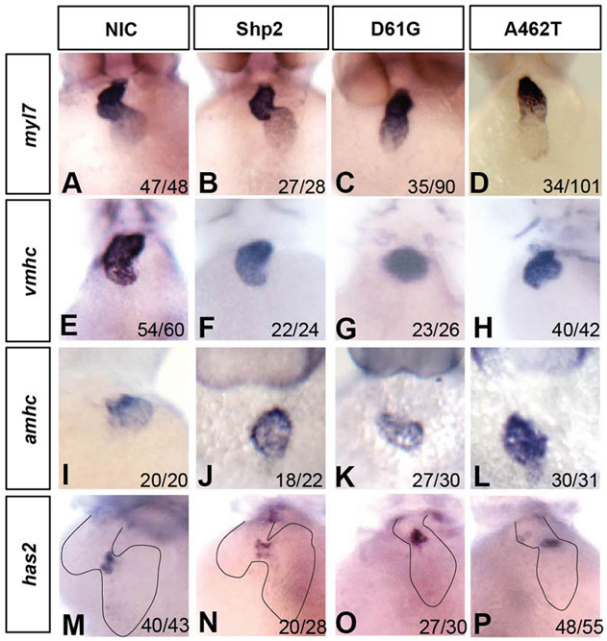

Fig. 2. Heart defects in embryos expressing Shp2-D61G and Shp2-A462T. Non-injected control embryos (NIC) and embryos injected at the one-cell stage with mRNA encoding WT-Shp2 (Shp2), Shp2-D61G or Shp2-A462T were fixed at 48 hpf and *in situ* hybridization was performed using probes for the myosin genes *myl7* (A-D, cardiomyocytes), *vmhc* (E-H, ventricle) and *amhc* (I-L, atrium), and for *has2* (M-P, endocardial cushions). Representative pictures are shown and the number of embryos showing this pattern/total number of embryos is indicated. The outline of the heart is indicated in M-P.

control and WT-Shp2-injected embryos (Fig. 2A-D). Myocardial chamber specification was not affected in NS-Shp2- and LS-Shp2-injected embryos, as determined by expression of *ventricular myosin heavy chain* (*vmhc*) (Fig. 2E-H) and *atrium myosin heavy chain* (*amhc*; *myh6* – Zebrafish Information Network) (Fig. 2I-L). Next, the formation of the endocardial cushions, from which the atrioventriclar valves will develop, was assessed by *has2* expression. In Shp2-D61G- and Shp2-A462T-expressing embryos, *has2* expression was not affected, compared with non-injected control and WT-Shp2-expressing embryos (Fig. 2M-P). Expression of this panel of markers was also assessed in embryos expressing Shp2-T73I (NS) and Shp2-G465A (LS) with similar results (supplementary material Fig. S2), indicating that all NS and LS variants induced similar defects. Taken together, these data indicate that expression of NS and LS variants of Shp2 led to a failure to undergo heart looping in a large proportion of the embryos, without inducing defects in cardiac chamber specification or endocardial cushion formation. In addition, the NS and LS variants of Shp2 induced cardiac defects to a similar extent during early development.

To investigate at which stage the cardiac defects arise in embryos expressing NS and LS variants of Shp2, *myl7* expression was analyzed at different time points of heart development, particularly during cardiac fusion and heart tube elongation. Zebrafish heart formation is initiated by fusion of two bilateral pools of cardiomyocytes at the 16-somite stage (16 hpf) into a cardiac disc at the midline of the embryo at 22 somites (20 hpf) (Yelon et al., 1999; Bakkers, 2011). No obvious defects were detected in *myl7* expression or cardiac fusion between non-injected control, WT-Shp2-, Shp2-D61G- and Shp2-A462T-expressing embryos up to 22 somites (Fig. 3A-H). At 28 hpf, the heart in WT-Shp2-expressing embryos formed a tube that extended from the midline to the area under the left eye (Fig. 3I), which resembled normal heart displacement. By contrast, in Shp2-D61G- and Shp2-A462T-expressing embryos, the displacement of the heart is randomized: 23% of Shp2-D61G-expressing embryos and 28% of Shp2-A462T-expressing embryos had a heart on the right, whereas 34% of Shp2-D61G-expressing embryos and 24% of Shp2-A462T-expressing embryos had their heart tube at the midline (Fig. 3J-L). Taken together, these results indicate that the first signs of cardiac abnormality in embryos expressing Shp2 variants are observed during asymmetric displacement of the heart tube.

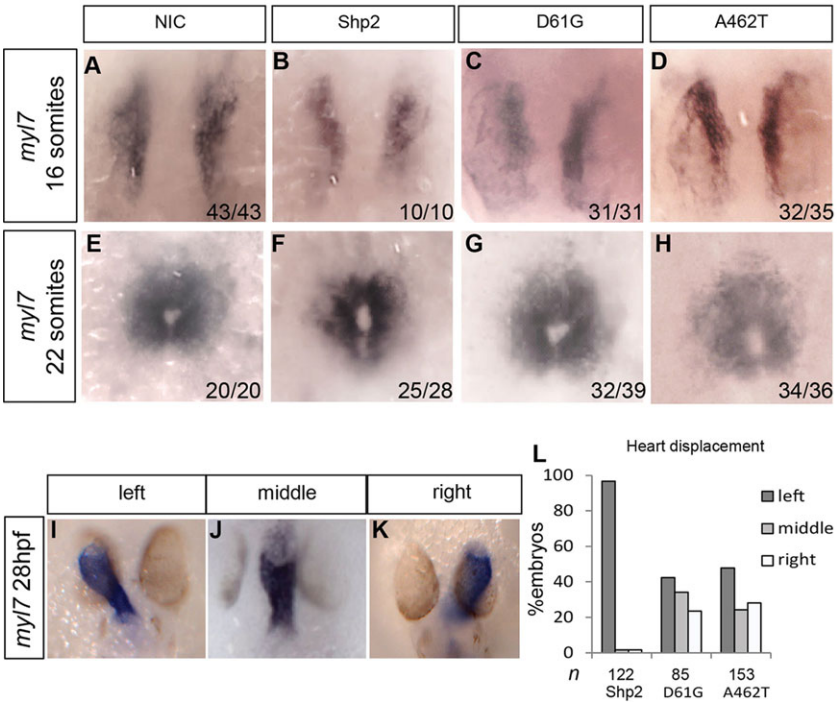

Fig. 3. Randomized heart displacement in response to expression of Shp2-D61G and Shp2-A462T. Embryos were injected at the one-cell stage with mRNA encoding WT-Shp2, Shp2-D61G or Shp2-A462T and fixed at the 16-somite stage, the 22-somite stage or at 28 hpf. *In situ* hybridization was carried out using a *myl7*-specific probe to mark cardiomyocytes. (A-H) The number of embryos displaying the depicted pattern/total number of embryos is indicated. (I-K) Representative pictures are shown displaying heart displacement to the left (I), middle (J) and right (K). (L) Percentages of left, middle and right cardiac displacement are depicted. The number of embryos (*n*) is indicated.

Development (2014) 141, 1961-1970 doi:10.1242/dev.106310

Decreased cardiomyocyte migration speed and rotation in embryos expressing NS and LS Shp2 variants

Randomization of heart displacement may be caused by compromised cardiomyocyte migration (Ramsdell, 2005). Tg(*myl7:*GFP) embryos express eGFP in cardiomyocytes and were used for high-resolution confocal time-lapse imaging to assess cardiomyocyte migration. As WT-Shp2-expressing embryos were indistinguishable from non-injected control embryos in *in situ* hybridization experiments (Figs 2 and 3), we used WT-Shp2-expressing embryos as a control for the embryos expressing NS and LS variants of Shp2 for subsequent experiments. Single cells were tracked in WT-Shp2-, Shp2-D61G- and Shp2-A462T-expressing embryos from cardiac disc stage (21 somites, 19.5 hpf) for 4 h and their velocities and directions were determined. Consistent with observations of heart morphogenesis in wild-type embryos (de Campos-Baptista et al., 2008; Smith et al., 2008), cardiac cells moved towards the left and anterior part of the embryo in WT-Shp2-expressing embryos (n=4). Cardiomyocytes in the posterior part of the cardiac disc moved faster than anterior cells (Fig. 4A-C). The Shp2-D61G- and Shp2-A462T-expressing embryos were imaged at 19.5 hpf, like the WT-Shp2-expressing embryos, and heart displacement was assessed subsequently at 24 hpf, allowing correlation between early migration defects and heart displacement. Embryos that displayed impaired heart displacement were selected for further analysis. It is noteworthy that none of the selected embryos displayed heart displacement to the right (Shp2-D61G, n=8; Shp2-A462T, n=8), which may be due to low penetrance of rightward heart displacement. Although cardiomyocytes in the selected embryos formed a cardiac tube, they showed reduced migration on the left. Representative images of an embryo expressing Shp2-A462T are depicted in Fig. 4D-F. Quantification of the speed of cardiomyocytes confirmed slower migration of cells in embryos expressing Shp2-D61G and Shp2-A462T, compared with WT-Shp2 (Fig. 4G). Cardiomyocytes in selected embryos expressing Shp2-D61G and Shp2-A462T did not cross the midline, but instead migrated anteriorly, which is consistent with defective heart displacement to the left. Rotation of the heart tube was quantified as described before and the observed 30° clockwise rotation of the cardiac cone in WT-Shp2-expressing embryos was consistent with the previously reported clockwise rotation in control embryos (Smith et al., 2008). Clockwise rotation was significantly decreased in embryos expressing Shp2-D61G and Shp2-A462T with impaired leftward heart displacement, compared with control WT-Shp2 (Fig. 4H). Our results indicate that directional cardiomyocyte migration and heart tube rotation is reduced in embryos expressing NS and LS Shp2 variants, which is consistent with the observed defects in heart tube displacement.

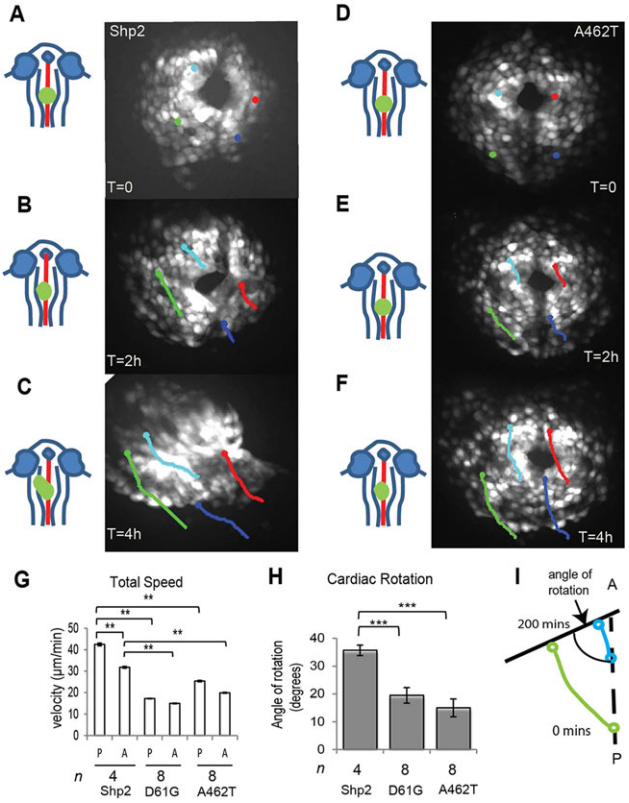

Fig. 4. Impaired cardiomyocyte migration in embryos expressing Shp2-D61G and Shp2-A462T. Embryos from the tg(*myl7:*GFP) line were injected with mRNA encoding WT-Shp2, Shp2-D61G or Shp2-A462T lacking eGFP-peptide 2A sequences to allow imaging of GFP-positive cardiomyocytes from the 22-somite stage onwards. (A-F) Representative individual GFP-positive cells were color-coded according to their location within the cardiac field at the 22-somite stage and tracked over a 200 min period. Dorsal view with anterior towards the top. Schematic representations of the embryos on the left indicate the position and shape of the heart in green. (A-C) WT-Shp2; (D-F) Shp2-A462T. (G) Quantification of the total speed of posterior (P) and anterior (A) cardiac progenitor cells. WT-Shp2-expressing embryos displayed normal leftward heart displacement; embryos expressing Shp2-D61G and Shp2-A462T that did not display normal heart displacement were selected for further analysis. (H) Clockwise cardiomyocyte rotation was determined of the same embryos as in G. Rotation was quantified as depicted in I. (G,H) Averages are indicated and error bars indicate s.e.m.; n indicates number of embryos. Statistical significance was determined using Student's t-test: $^{**}P<0.01$ and $^{***}P<0.001$.

NS and LS Shp2 variants disrupt left/right asymmetry

To determine whether the loss of asymmetry in the hearts of embryos expressing NS and LS Shp2 variants is associated with disruption of overall L/R asymmetry, we analyzed the expression of a number of laterality markers. southpaw (*spaw*) is one of the earliest markers displaying asymmetric expression in development (Long et al., 2003). *spaw* was predominantly expressed in the left lateral plate mesoderm (LPM) in WT-Shp2-expressing embryos (Fig. 5A). *spaw* expression was affected in embryos expressing Shp2-D61G and Shp2-A462T, compared with WT-Shp2, in that 23% of Shp2-D61G- and 17% of Shp2-A462T-expressing embryos displayed bilateral *spaw* expression and 26% of Shp2-D61G- and 28% of Shp2-A462T-expressing embryos expressed *spaw* exclusively in the right LPM (Fig. 5B-D). Next, expression of *lefty2* (*lft2*), a downstream target of *spaw*, was investigated at the 22-somite stage (20 hpf). In WT-Shp2-expressing embryos, *lft2* was detected in the left cardiac field in all cases (Fig. 5E). By contrast, expression of *lft2* in Shp2-D61G- and Shp2-A462T-expressing embryos was randomized. 30% of the Shp2-D61G-expressing embryos expressed *lft2* on the right side (Fig. 5E-G). Similarly, in Shp2-A462T-expressing embryos, *lft2* expression was detected at the right side in 42% of the embryos. *spaw* is required for visceral organ L/R asymmetry (Long et al., 2003), suggesting that defects in L/R asymmetry may not be limited to the heart in embryos expressing Shp2 variants. To investigate this, the position of the liver was assessed by analysis of the expression of *fabp*. *fabp* expression was randomized at 48 hpf in embryos expressing Shp2-D61G and Shp2-A462T, in that the liver developed on the opposite side in 20% of the Shp2-D61G-expressing embryos and 24% of the Shp2-A462T-expressing embryos, or on both sides in 18% of the Shp2-D61G- and 9% of the Shp2-A462T-expressing embryos (Fig. 5H-K). In control WT-Shp2-expressing embryos, the liver always developed on the left side of the embryos. Analysis of the embryonic midline using the

Development (2014) 141, 1961-1970 doi:10.1242/dev.106310

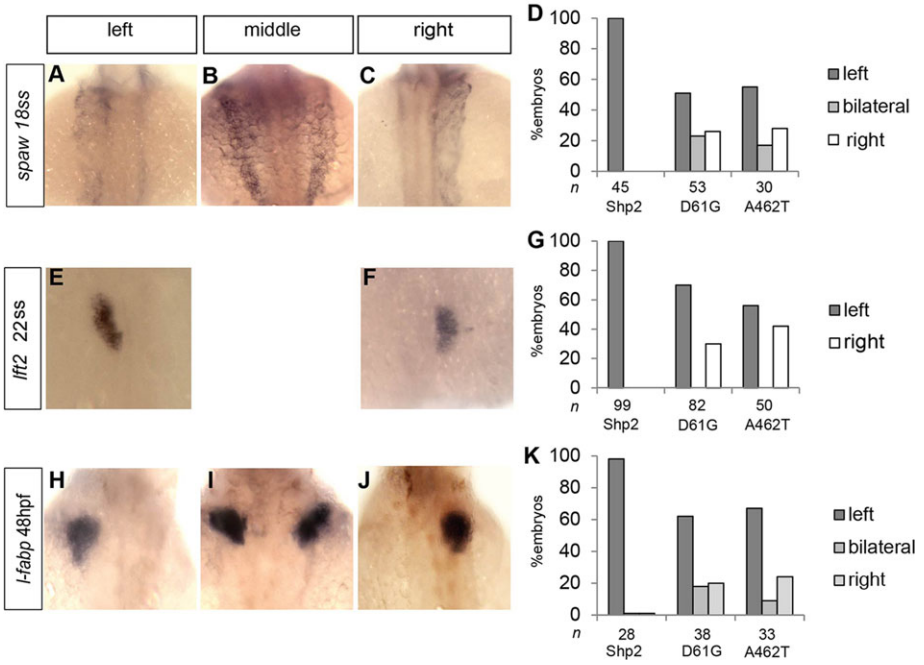

Fig. 5. Expression of Shp2-D61G- and Shp2-A462T-induced L/R asymmetry defects. Embryos were injected at the one-cell stage with mRNA encoding WT-Shp2 (Shp2), Shp2-D61G or Shp2-A462T and fixed at the stage indicated. *In situ* hybridization was carried out using probes specific for *spaw* (A-D, *southpaw*), *lft2* (E-G, *lefty2*) and *fabp* (H-K, fatty acid binding protein, marking the liver). Representative pictures are shown of Shp2-D61G-expressing embryos. *lft2* expression was observed only on the left side or on the right side. Organ asymmetry as assessed using the different markers was scored for embryos injected with WT-Shp2, Shp2-D61G and Shp2-A462T. Percentages of left, middle/bilateral and right expression of the markers are depicted. The number of embryos (*n*) is indicated.

sonic hedgehog marker (Krauss et al., 1993) indicated that expression of Shp2-D61G and Shp2-A462T altered left-right patterning without disrupting the midline, which provides a barrier between the left and the right side (supplementary material Fig. S4). These results show that L/R patterning in the LPM is impaired in embryos expressing NS and LS Shp2 variants, which may lead to randomization of heart and gut laterality.

Ciliogenesis and cilia function in Kupffer's vesicle are impaired in embryos expressing NS and LS Shp2-variants

It is well established that Kupffer's vesicle (KV), a fluid-filled ciliated organ, is involved in the establishment of L/R asymmetry in zebrafish (Neugebauer et al., 2009; Liu et al., 2011). Through the oriented rotation of the cilia inside the KV, asymmetric expression of genes such as *spaw* and *lft2* is established. Immunohistochemistry was carried out using an acetylated tubulin antibody to detect cilia in the KV of 10-somite stage embryos (14 hpf) (Fig. 6A-C). The mean number of cilia was 51.4±0.5 in WT-Shp2-expressing embryos, whereas in embryos expressing Shp2-D61G and Shp2-A462T, the number of cilia was significantly reduced to 30.4±0.7 and 28.5±0.4, respectively (n=10 embryos each) (Fig. 6D). In addition, the cilia length was significantly reduced in embryos expressing NS and LS Shp2 variants (both 3.2±0.1 µm, n=241 cilia for Shp2-D61G and n=172 cilia for Shp2-A462T, respectively) compared with control (4.2±0.1 µm, n=379 cilia for WT-Shp2) (Fig. 6E). Measurements of the area of KV indicated significant differences in lumen size among wild-type (4517±355 µm^2, n=10), Shp2-D61G (2243±190 µm^2, n=10) and Shp2-A462T (1914±256 µm^2, n=10) embryos (Fig. 6F). These results suggest that disruption of L/R asymmetry in embryos expressing NS and LS variants of Shp2 was a consequence of defective KV function, resulting from impaired ciliogenesis in the KV. To determine the KV functionality directly, we analyzed the fluid flow in embryos expressing NS and LS variants of Shp2. Tracking of fluorescent beads injected into the KV lumen of wild-type Shp2-expressing embryos showed counterclockwise rotation of the beads (Fig. 6G). By contrast, tracking of the beads in Shp2-D61G- and Shp2-A462T-expressing embryos showed that the beads moved about randomly (Fig. 6H-I), indicating a loss of coordinated flow. In addition, beads tracked in Shp2-D61G and Shp2-A462T-expressing embryos showed a strongly reduced average flow velocity relative to wild-type Shp2-expressing embryos (Fig. 6M). These results indicate that ciliogenesis and cilia function is impaired in the KV of embryos expressing NS and LS variants of Shp2, resulting in defective KV function.

Early treatment with the MEK inhibitor CI-1040 rescued L/R asymmetry, heart asymmetry and KV function in embryos expressing NS and LS Shp2 variants

Shp2 variants enhance RAS/MAPK signaling (Feng, 1999). Previously, we and others showed that inhibition of MEK rescued developmental defects in zebrafish embryos that were caused by expression of activators of the RAS/MAPK pathway (Anastasaki et al., 2009; Runtuwene et al., 2011). We investigated whether inhibition of MEK would also rescue the cardiac defects in embryos expressing NS and LS Shp2 variants. First, the efficacy of the MEK inhibitor CI-1040 to rescue early developmental defects was assessed. Expression of Shp2-D61G or Shp2-A462T in zebrafish embryos induced cell movement defects, resulting in elongated embryos at bud stage (10 hpf) (Fig. 7A-C). Treatment with 0.25 µM CI-1040 at 4.5 hpf for 1 h rescued development at 10.5 hpf of embryos expressing Shp2-D61G and Shp2-A462T (Fig. 7D-F). Quantification of the epiboly defects confirmed the rescue of the embryos expressing NS and LS Shp2 variants (Fig. 7G). In addition, we confirmed that elevated pERK levels in embryos expressing Shp2-D61G and Shp2-A462T were reduced by CI-1040-mediated inhibition of MEK at 10 hpf (Fig. 7H).

Next, the effect of CI-1040 treatment was assessed on asymmetry of the heart in embryos expressing Shp2-D61G and Shp2-A462T. Treatment with 0.25 µM CI-1040 at 4.5 hpf for 1 h rescued leftward displacement of the heart at 24 hpf of Shp2-D61G and Shp2-A462T-expressing embryos (Fig. 7I,J). However, treatment of these embryos for 1 h with CI-1040 at the 10-somite stage (14 hpf) did not restore normal heart displacement in embryos expressing NS and LS Shp2 variants (Fig. 7K). Treatment with 0.25 µM CI-1040 at 4.5 hpf for 1 h largely rescued randomization of the left-right asymmetry markers and of the liver (supplementary material Fig. S5). These results

Development (2014) 141, 1961-1970 doi:10.1242/dev.106310

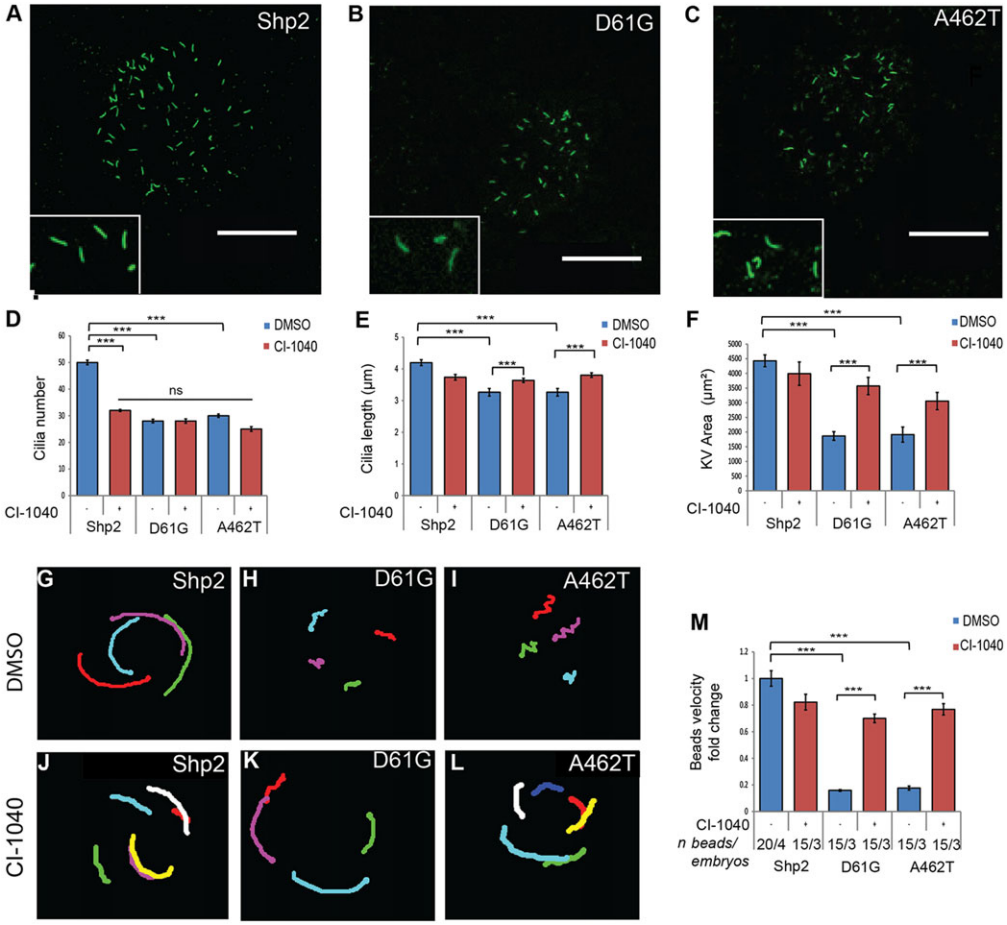

Fig. 6. Impaired ciliogenesis and cilia function in Kupffer's vesicle in embryos expressing Shp2-D61G and Shp2-A462T. (A-C) Immunohistochemistry was carried out using anti-acetylated tubulin on WT-Shp2-, Shp2-D61G- or Shp2-A462T-expressing embryos that were fixed at the 10-somite stage. Representative confocal images are depicted here. Scale bars: 50 μm. Insets show close-ups of cilia. (D-F) Quantification of the cilia number, cilia length and KV area in WT-Shp2-, Shp2-D61G- and Shp2-A462T-expressing embryos that were treated with 0.5% DMSO (control) or 0.25 μM CI-1040 at 4.5 hpf for 1 h and fixed at the 10-somite stage (n=10 for each condition). Averages are depicted with error bars indicating s.e.m. Statistical significance was determined using Student's t-test: ***P<0.001; **P<0.01. (G-L) Tracks of fluorescent beads injected in KV. (G-L) Maximum projections of fluorescent bead movements injected in the KV of WT-Shp2-, Shp2-D61G- or Shp2-A462T-expressing embryo that were treated with 0.5% DMSO or 0.25 μM CI-1040 at 4.5 hpf for 1 h and fixed at the 10-somite stage. (M) Average flow velocity of beads in KV of embryos expressing WT-Shp2, Shp2-D61G and Shp2-A462T without (–) or with (+) CI-1040 treatment. The number of beads/number of embryos that were analyzed is indicated. Averages are depicted with error bars indicating s.e.m. Statistical significance was determined using Student's t-test: ***P<0.001.

indicate that inhibition of MEK at early stages rescues L/R asymmetry in embryos expressing NS and LS Shp2-variants.

Finally, the effect of CI-1040 treatment on ciliogenesis and cilia function in KV was assessed. The cilia number was not rescued upon treatment with 0.25 μM CI-1040 at 4.5 hpf for 1 h. In fact, the cilia number in CI-1040-treated WT-Shp2-expressing embryos was significantly reduced to similar levels as in CI-1040-treated embryos expressing NS or LS variants of Shp2 (Fig. 6D). Yet, CI-1040 treatment rescued cilia length in embryos expressing Shp2 variants (3.6±0.1 μm in Shp2-D61G- and 3.8±0.1 μm in Shp2-A462T-expressing embryos, compared with 3.2±0.1 μm in untreated embryos) (Fig. 6E). Cilia length in WT-Shp2-expressing embryos was reduced somewhat in response to CI-1040 treatment (from 4.2±0.1 μm to 3.7±0.1 μm; Fig. 6E) and hence, CI-1040 treatment abolished the difference in cilia length between embryos expressing WT-Shp2 and Shp2 variants. Moreover, CI-1040 treatment rescued KV area (3736±373 μm^2 in Shp2-D61G- and 3055±294 μm^2 in Shp2-A462T-expressing embryos, compared with 3986±398 μm^2 in WT-Shp2-expressing embryos; Fig. 6F). Importantly, treatment with 0.25 μM CI-1040 at 4.5 hpf rescued the counterclockwise rotation of the fluorescent beads in Shp2-D61G- and Shp2-A462T-expressing embryos to levels that were similar to those in WT-Shp2-expressing embryos (Fig. 6J-M). Taken together, these results suggest that the cardiac defects in zebrafish embryos expressing NS and LS Shp2 variants are due to hyperactivate MAPK-induced laterality defects originating from impaired cilia function in KV.

DISCUSSION

In this paper, we used zebrafish to investigate defects in cardiac development in response to expression of NS and LS variants of Shp2. We found that NS- and LS-Shp2-expressing embryos showed impaired leftward heart displacement. Our results are consistent with a report that Noonan-associated mutations induce a cardiac looping defect in *Xenopus* (Langdon et al., 2012). Here, we provide insight into the underlying mechanism. The cardiac defects that we observed in zebrafish embryos are associated with L/R laterality defects and with defects in ciliogenesis. Expression of NS and LS variants of Shp2 in zebrafish embryos enhanced MAPK activation. The laterality defects were rescued by early treatment with CI-1040,

Development (2014) 141, 1961-1970 doi:10.1242/dev.106310

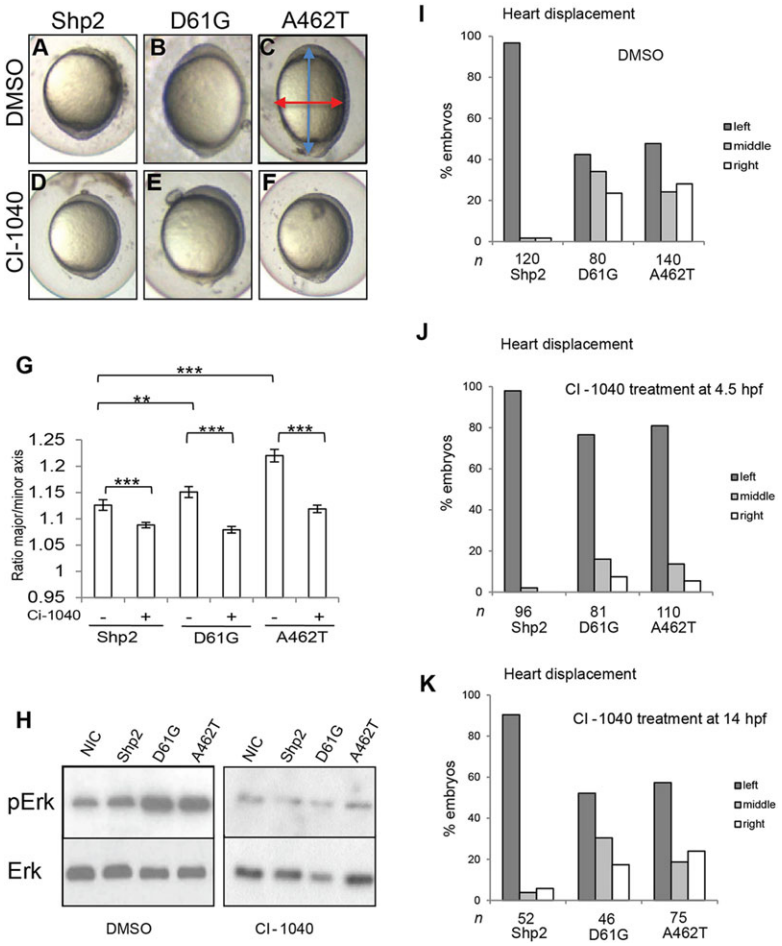

Fig. 7. Early treatment with the MEK-inhibitor CI-1040 rescued leftward heart displacement and cilia length in embryos expressing NS and LS Shp2 variants. Embryos were injected with mRNA encoding WT-Shp2 (Shp2), Shp2-D61G and Shp2-A462T at the one-cell stage. (A-F) Representative images of bud stage embryos are depicted. The shape of the NS- and LS-Shp2-expressing embryos is restored by treatment with 0.25 μM CI-1040 at 4.5 hpf for 1 h. (G) The ratio between the length of the major and minor axes was determined as quantitative measure of the epiboly defects in NS- and LS-Shp2-expressing embryos. Averages are depicted with error bars indicating s.e.m. Statistical significance was determined using Student's *t*-test (***P*<0.01; ****P*<0.001). (H) Embryos were treated with MEK inhibitor CI-1040 (0.25 μM) for 1 h at 4.5 hpf or mock-treated with DMSO and lysed at 10 hpf. Immunoblots of the zebrafish lysates were stained using antibodies specific for pErk and Erk. The experiment was repeated three times and representative blots are depicted here. (I-K) Embryos were mock treated with DMSO (I) or with CI-1040 for 1 h at 4.5 hpf (J) or at 10 hpf (K). Heart displacement was determined in embryos following *in situ* hybridization with a *myl7*-specific probe as in Fig. 4. Histograms represent the percentage of embryos with heart displacement to the left, middle or right. The total number of embryos (*n*) is indicated.

a MEK inhibitor, indicating that the defects in heart asymmetry were caused by enhanced MAPK signaling before gastrulation.

Here, we focused on the cardiac defects in embryos expressing NS and LS Shp2 variants. The heart defects only became evident during cardiac tube formation, the first asymmetric process that occurs in the zebrafish heart (Bakkers, 2011). Normally, the cardiac tube is displaced to the left, but in embryos expressing NS and LS Shp2 variants, heart displacement was randomized (Fig. 3). Cell movement analyses revealed a delay in cell movements, coupled with reduced cardiac tube rotation, resulting in morphologically abnormal hearts at 28 hpf (Fig. 4). Cell tracking studies showed that loss of Nodal or BMP signaling leads to similar defects (de Campos-Baptista et al., 2008; Smith et al., 2008). Nodal mutant embryos show reduced speed and directional movement of the cardiomyocytes, resulting in disruption of the leftward morphogenesis and cardiac cone rotation. Asymmetric *spaw* expression in the LPM is responsible for the correct displacement of the heart tube to the left (Long et al., 2003; de Campos-Baptista et al., 2008). In line with these findings, we found that expression of *spaw* was randomized in embryos expressing NS and LS Shp2 variants, concomitant with its downstream gene target *lft2*. As a consequence, left/right asymmetry was lost and leftward displacement of the heart in embryos expressing Shp2-D61G and Shp2-A462T was compromised. In addition, randomized *fabp* expression suggested that not only asymmetry of the heart, but also of the liver was impaired.

Left-right asymmetry is conserved across species and defects in left-right asymmetry are collectively called laterality disease (Mercola and Levin, 2001). The phenotype we observed in zebrafish embryos expressing NS and LS Shp2 variants was characterized by randomization of left/right asymmetry. It is noteworthy that laterality disease is frequently associated with congenital heart defects (CHDs) (Ramsdell, 2005). Impaired left-right patterning can affect cardiac morphogenesis, resulting in defective septation and/or double outlet right ventricle (DORV) (Ramsdell, 2005). Cardiac defects associated with laterality diseases are also reported in Shp2-D61G knock-in mice. A proportion of the heterozygous Shp2-D61G mice displays septal defects and DORV (Araki et al., 2004). However, laterality defects are not the only cause of septation defects or DORV. Other laterality defects were not reported in NS or LS Shp2 knock-in mice, and laterality defects have not been commonly reported in humans with NS and LS. Hence, it remains to be determined whether laterality defects have a role in human NS and LS.

In zebrafish expressing NS and LS variants of Shp2, we found that the underlying mechanism for randomization of L/R asymmetry is likely impaired cilia function in the KV. In particular, cilia length and KV area were associated with Shp2 variant-induced impaired fluid flow in KV and subsequent loss of asymmetry (Fig. 6). It is well established that L/R asymmetry is mediated by cilia that generate fluid flow within the KV, resulting in expression of *spaw* in the left side of the LPM (Nonaka et al., 1998; Essner et al., 2005). Laser-mediated ablation of KV randomizes expression of *spaw* and *lft2* (Essner et al., 2005). Moreover, shorter cilia result in perturbed intravesicular fluid flow, leading to loss of asymmetry in the heart, brain and viscera (Ferrante et al., 2009). KV formation is completed by the 6-somite

Development (2014) 141, 1961-1970 doi:10.1242/dev.106310

stage (12 hpf) (Oteiza et al., 2008, 2010) and the generation of the KV depends on the dorsal forerunner cells (DFCs) that are induced during the blastula period (Alexander et al., 1999). Defects in the specification, clustering or organization of DFCs induce defective KV organogenesis and/or ciliogenesis (Essner et al., 2005; Oteiza et al., 2010). Therefore, it will be interesting to investigate the role of the NS and LS Shp2 variants in DFC biology.

Shp2 is a well-known downstream factor in FGFR signaling (Neel and Tonks, 1997). It has been reported that FGFR1 signaling regulates cilia length in zebrafish. Morpholino (MO)-mediated knockdown of FGFR1 in zebrafish reduces cilia length in KV and perturbs directional fluid flow, thus impairing L/R patterning of the embryo (Neugebauer et al., 2009). The observation that knockdown of FGFR1, a positive regulator of MAPK signaling, has similar effects to mutant Shp2-induced hyperactivation of MAPK appears to be contradictive. However, it is not uncommon that attenuation and activation of a signaling pathway have the same effect on developmental processes. FGFR1 knockdown, on the one hand, and Shp2 variant-mediated enhanced MAPK activation, on the other, have similar effects on cilia function in KV and both impair L/R asymmetry. Our results predict that ectopic activation of MAPK signaling, e.g. overexpression of (activated) MAPK, around gastrulation would also induce laterality defects.

Defective ciliogenesis was observed in the KV of NS and LS-Shp2-expressing embryos. It remains to be determined whether ciliogenesis in other organs is also affected in these embryos. It is noteworthy that deafness is associated with LS in humans. Deafness is typically associated with defective cilia in the inner ear and future work should focus on ciliogenesis in organs other than KV in NS and LS Shp2-variant-expressing zebrafish embryos.

The cardiac defects that were induced by expression of NS and LS Shp2 variants in zebrafish embryos were indistinguishable. MAPK activation was elevated at bud stage in response to expression of both Shp2-D61G (NS) as well as Shp2-A462T (LS) (Fig. 7H), which might explain why we observed similar developmental defects at early stages. It is well established that NS-Shp2 mutations enhance MAPK activation, but LS-Shp2 often does not activate MAPK signaling. Nevertheless, it is not unprecedented that LS mutations induce defects that are associated with activation of MAPK signaling. Expression of LS-Shp2 mutants in *Drosophila* results in ectopic wing veins and a rough eye phenotype, characteristics of increased Erk activation. This gain-of-function phenotype is similar to that of NS-Shp2 transgenic flies (Oishi et al., 2006, 2009). Moreover, a recent study shows that induced pluripotent stem cells (iPSCs) derived from the fibroblasts of individuals with LS display higher basal pERK levels compared with those of control iPSCs (Carvajal-Vergara et al., 2010). How the NS and LS variants of Shp2 would both activate MAPK signaling remains to be determined. Whereas catalytic activity of Shp2 is enhanced by the NS mutations, it is reduced by the LS mutations, indicating that MAPK activation is not directly affected by alterations in Shp2 catalytic activity. Rather, the NS and LS Shp2-variant-induced defects may result from a phosphatase-independent function of Shp2. Alternatively, as suggested in a recent report, the LS variants of SHP2 retain some catalytic activity and mediate gain-of-function phenotypes, because they have an increased propensity for the open conformation. Thus, the LS variants bind upstream activators preferentially and stay in complex with their scaffolding adapters longer, thus prolonging specific substrate turnover (Yu et al., 2013), which in turn may lead to MAPK activation.

Whereas MAPK activation may be elevated by both NS and LS variants of Shp2, elevated PI3K/AKT signaling is exclusively associated with LS. Hyperactivation of AKT signaling in response to LS-Shp2 is responsible for HCM in mouse hearts (Ishida et al., 2011; Marin et al., 2011; Schramm et al., 2012). We also observed elevated pAkt levels in response to LS-Shp2 in zebrafish embryos (supplementary material Fig. S3), but we did not observe HCM in these embryos. The cardiac defects in embryos expressing NS and LS Shp2 variants were indistinguishable. Moreover, these heart defects were rescued by early treatment with the MEK inhibitor to a similar extent, indicating a causal role for elevated MAPK activation in the observed cardiac defects, independently of Akt signaling.

In summary, our data provide new insights into the role of pathogenic Shp2 variants in cardiac development. Expression of NS and LS Shp2 variants led to similar cardiac defects in zebrafish that were associated with impaired L/R asymmetry, resulting from impaired cilia function in KV. Treatment with a MEK inhibitor prior to gastrulation rescued cilia function, L/R asymmetry and heart displacement, suggesting a causal relation with enhanced MAPK signaling. No studies to date have examined the effect of NS and LS Shp2 variants on L/R asymmetry. Our paper opens a new prospective in understanding how pathogenic SHP2 and downstream MAPK activation relates to cardiac development through its effects on L/R asymmetry.

MATERIALS AND METHODS

Fish line

Zebrafish were maintained and the embryos were staged as previously described (Kimmel et al., 1995). The tg(*myl7*:GFP) line has been previously described (Chocron et al., 2007). All procedures involving experimental animals were approved by the local animal experiments committee and performed in compliance with local animal welfare laws, guidelines and policies, according to national and European law.

Constructs, RNA and injections

The eGFP-peptide 2A-Shp2 construct was derived by PCR. 5′ capped sense mRNAs were synthesized using the mMessage mMachine kit (Ambion) and linearized plasmid DNA. mRNA injections were performed at the one-cell stage as described previously (Hyatt and Ekker, 1999) using optimized amounts of mRNA (D61G=150 pg, A465T=50 pg, T73I=80 pg G465A=100 pg, WT-Shp2=150 pg).

Immunoblotting

Zebrafish embryos (10 hpf) were lysed in buffer containing 50 mM Tris (pH 7.5), 150 mM NaCl, 1 mM EDTA, 1 mM sodium orthovanadate, 1% Nonidet P-40, 0.1% sodium deoxycholate, protease inhibitor mixture (Complete Mini, Roche Diagnostics) and vanadate. Samples were run on SDS-PAGE gel (10%), transferred to PVDF membrane and stained with Coomassie Blue to verify equal loading. The blots were probed with antibodies specific for SHP2, Actin, pERK, ERK, pAKT, AKT (all Cell Signaling) and GFP (Torrey Pines). Detection was carried out using enhanced chemiluminescence (Thermo Scientific kit).

In situ hybridization and immunofluorescence microscopy

In situ hybridization was carried out essentially as described (Thisse et al., 1993) using probes specific for, *myl7* (Yelon et al., 1999), *vmhc* (Yelon, 2001), *amhc* (Smith et al., 2009), *has2* (Bakkers et al., 2004), *lefty2* (Bisgrove et al., 1999), *southpaw* (Long et al., 2003), *fabp* and *shh* (Krauss et al., 1993).

For zebrafish immunohistochemistry, embryos were fixed in 4% DENT's solution (20% dimethylsulfoxide/80% methanol) at 4°C, and subsequently blocked for 1 h in PBS containing 5% lamb serum, 1% BSA, 1% DMSO and 0.1% Triton-X. Embryos were incubated in mouse anti-acetylated tubulin (1:500, Sigma) for 3 h at room temperature. After extensive washing, embryos were incubated in goat anti-mouse Alexa Fluor 488. Embryos were

Development (2014) 141, 1961-1970 doi:10.1242/dev.106310

flat-mounted in glycerol. Images were acquired using an SPE laser-scanning confocal microscope. Confocal *z*-series images were assembled to present the sum of the focal planes; cilia length, cilia number and KV lumen area were manually measured using ImageJ software (http://rsb.info.nih.gov/ij/).

Pharmacological inhibition of MAPK signaling

To test the prevention of the NS/LS Shp2 mRNA phenotype, embryos injected with NS/LS Shp2 mRNA were incubated with 0.25 µM CI-1040 at 4.5 hpf or 10 hpf for 1 h at 28.5°C in the dark.

Time-lapse imaging and analysis

Embryos at the 22-somite stage were dechorionated and mounted in glass-bottom six-well plates using 0.25% agarose in E3 embryo medium containing 16 mg/ml 3-amino benzoic acid ethylester to block contractile movements. Confocal imaging was performed using a spinning disc confocal laser scanning microscope with 20× magnification, acquiring stacks every 5 min. Embryos were kept at 28.5°C during recordings. ImageJ software (http://rsb.info.nih.gov/ij/) was used to generate time-lapse movies and for cell counting. Cell tracking was carried out using Volocity software (Improvision) followed by manual inspection of individual tracks generating quantification of total speed (track length/time). Rotation was calculated by measuring the angle with the LR axis of four imaginary lines connecting four individual cells at the start and the end of the time-lapse (200 min). All statistical analyses were performed in Excel (Microsoft) using the two-tailed Student's *t*-test.

KV fluid flow and cilia motility

Fluorescent beads (Polysciences) were injected into KV to visualize flow as described previously (Essner et al., 2005). Bead flow was imaged at the 8- to 10-somite stage (SS) on a Leica AF7000 microscope (Leica Microsystems GmbH, Wetzlar, Germany) using a 63× water dipping objective and an Hamamatsu C9300-221 high-speed CCD camera (Hamamatsu Photonics, Hamamatsu City, Japan) at 80 fps to record a 10 s movie. Movies were generated using ImageJ software. Bead tracking was carried out using Volocity software (Improvision). For each embryo, four or five beads were tracked for a minimum of 50 frames of the movie and the average bead velocity was calculated.

High-speed imaging and analysis

Embryos (2 dpf) were mounted in 0.25% agarose prepared in E3 medium embryonic medium with 16 mg/ml 3-amino benzoic acid ethylester. Embryonic hearts were imaged with a Hamamatsu C9300-221 high-speed CCD camera (Hamamatsu Photonics, Hamamatsu City, Japan) at 150 fps mounted on a Leica AF7000 microscope (Leica Microsystems GmbH, Wetzlar, Germany) in a controlled temperature chamber (28.5°C) using Hokawo 2.1 imaging software (Hamamatsu Photonics GmbH, Herrsching am Ammersee, Germany). Image analysis was carried out with ImageJ (http://rsbweb.nih.gov/ij/). Statistical analysis and drawing of the box-whisker plot were carried out in Excel 2007 (Microsoft, Redmond, WA, USA).

Statistics

Cilia measurements were analyzed using the two-tailed Student's *t*-test. Averages for controls and experimental were compared within each clutch of embryos. Results were considered significant when $P<0.05$ and results are expressed as mean±s.e.m. (*$P<0.05$, **$P<0.01$, ***$P<0.001$).

Competing interests

The authors declare no competing financial interests.

Author contributions

J.d.H. conceived the project; M.B. and J.d.H. designed the approach with help from F.T., E.N. and J.B.; M.B., J.P.O., F.T. and E.N. performed experiments; M.B. and J.d.H. prepared the manuscript, which was edited by J.P.O., F.T., E.N. and J.B. prior to submission.

Funding

This work was funded, in part, by a grant from the Research Council for Earth and Life Sciences [ALW 819.02.021] with financial aid from the Netherlands Organisation for Scientific Research (NWO) (to J.d.H.). Deposited in PMC for immediate release.

Supplementary material

Supplementary material available online at
http://dev.biologists.org/lookup/suppl/doi:10.1242/dev.106310/-/DC1

References

Alexander, J., Rothenberg, M., Henry, G. L. and Stainier, D. Y. R. (1999). casanova plays an early and essential role in endoderm formation in zebrafish. *Dev. Biol.* **215**, 343-357.

Allanson, J. E. and Roberts, A. E. (1993). Noonan syndrome. In *GeneReviews* (ed. R. A. Pagon,, M. P. Adam, T. D. Bird, C. R. Dolan, C. T. Fong and K. Stephens). University of Washington: Seattle, WA.

Anastasaki, C., Estep, A. L., Marais, R., Rauen, K. A. and Patton, E. E. (2009). Kinase-activating and kinase-impaired cardio-facio-cutaneous syndrome alleles have activity during zebrafish development and are sensitive to small molecule inhibitors. *Hum. Mol. Genet.* **18**, 2543-2554.

Araki, T., Mohi, M. G., Ismat, F. A., Bronson, R. T., Williams, I. R., Kutok, J. L., Yang, W., Pao, L. I., Gilliland, D. G., Epstein, J. A. et al. (2004). Mouse model of Noonan syndrome reveals cell type- and gene dosage-dependent effects of Ptpn11 mutation. *Nat. Med.* **10**, 849-857.

Bakkers, J. (2011). Zebrafish as a model to study cardiac development and human cardiac disease. *Cardiovasc. Res.* **91**, 279-288.

Bakkers, J., Kramer, C., Pothof, J., Quaedvlieg, N. E. M., Spaink, H. P. and Hammerschmidt, M. (2004). Has2 is required upstream of Rac1 to govern dorsal migration of lateral cells during zebrafish gastrulation. *Development* **131**, 525-537.

Bisgrove, B. W., Essner, J. J. and Yost, H. J. (1999). Regulation of midline development by antagonism of lefty and nodal signaling. *Development* **126**, 3253-3262.

Carvajal-Vergara, X., Sevilla, A., D'Souza, S. L., Ang, Y.-S., Schaniel, C., Lee, D.-F., Yang, L., Kaplan, A. D., Adler, E. D., Rozov, R. et al. (2010). Patient-specific induced pluripotent stem-cell-derived models of LEOPARD syndrome. *Nature* **465**, 808-812.

Chan, R. J. and Feng, G.-S. (2007). PTPN11 is the first identified proto-oncogene that encodes a tyrosine phosphatase. *Blood* **109**, 862-867.

Chocron, S., Verhoeven, M. C., Rentzsch, F., Hammerschmidt, M. and Bakkers, J. (2007). Zebrafish Bmp4 regulates left-right asymmetry at two distinct developmental time points. *Dev. Biol.* **305**, 577-588.

de Campos-Baptista, M. I. M., Holtzman, N. G., Yelon, D. and Schier, A. F. (2008). Nodal signaling promotes the speed and directional movement of cardiomyocytes in zebrafish. *Dev. Dyn.* **237**, 3624-3633.

De Rocca Serra-Nedelec, A., Edouard, T., Treguer, K., Tajan, M., Araki, T., Dance, M., Mus, M., Montagner, A., Tauber, M., Salles, J.-P. et al. (2012). Noonan syndrome-causing SHP2 mutants inhibit insulin-like growth factor 1 release via growth hormone-induced ERK hyperactivation, which contributes to short stature. *Proc. Natl. Acad. Sci. U.S.A.* **109**, 4257-4262.

Digilio, M. C., Conti, E., Sarkozy, A., Mingarelli, R., Dottorini, T., Marino, B., Pizzuti, A. and Dallapiccola, B. (2002). Grouping of multiple-lentigines/LEOPARD and Noonan syndromes on the PTPN11 gene. *Am. J. Hum. Genet.* **71**, 389-394.

Edouard, T., Combier, J. P., Nedelec, A., Bel-Vialar, S., Metrich, M., Conte-Auriol, F., Lyonnet, S., Parfait, B., Tauber, M., Salles, J. P. et al. (2010). Functional effects of PTPN11 (SHP2) mutations causing LEOPARD syndrome on epidermal growth factor-induced phosphoinositide 3-kinase/AKT/glycogen synthase kinase 3beta signaling. *Mol. Cell. Biol.* **30**, 2498-2507.

Essner, J. J., Amack, J. D., Nyholm, M. K., Harris, E. B. and Yost, H. J. (2005). Kupffer's vesicle is a ciliated organ of asymmetry in the zebrafish embryo that initiates left-right development of the brain, heart and gut. *Development* **132**, 1247-1260.

Feng, G.-S. (1999). Shp-2 tyrosine phosphatase: signaling one cell or many. *Exp. Cell Res.* **253**, 47-54.

Feng, G. S., Hui, C. C. and Pawson, T. (1993). SH2-containing phosphotyrosine phosphatase as a target of protein-tyrosine kinases. *Science* **259**, 1607-1611.

Ferrante, M. I., Romio, L., Castro, S., Collins, J. E., Goulding, D. A., Stemple, D. L., Woolf, A. S. and Wilson, S. W. (2009). Convergent extension movements and ciliary function are mediated by ofd1, a zebrafish orthologue of the human oral-facial-digital type 1 syndrome gene. *Hum. Mol. Genet.* **18**, 289-303.

Freeman, R. M., Jr, Plutzky, J. and Neel, B. G. (1992). Identification of a human src homology 2-containing protein-tyrosine-phosphatase: a putative homolog of Drosophila corkscrew. *Proc. Natl. Acad. Sci. U.S.A.* **89**, 11239-11243.

Hanna, N., Montagner, A., Lee, W. H., Miteva, M., Vidal, M., Vidaud, M., Parfait, B. and Raynal, P. (2006). Reduced phosphatase activity of SHP-2 in LEOPARD syndrome: consequences for PI3K binding on Gab1. *FEBS Lett.* **580**, 2477-2482.

Hof, P., Pluskey, S., Dhe-Paganon, S., Eck, M. J. and Shoelson, S. E. (1998). Crystal structure of the tyrosine phosphatase SHP-2. *Cell* **92**, 441-450.

Huyer, G. and Alexander, D. R. (1999). Immune signalling: SHP-2 docks at multiple ports. *Curr. Biol.* **9**, R129-R132.

Hyatt, T. M. and Ekker, S. C. (1999). Vectors and techniques for ectopic gene expression in zebrafish. *Methods Cell Biol.* **59**, 117-126.
Ishida, H., Kogaki, S., Narita, J., Ichimori, H., Nawa, N., Okada, Y., Takahashi, K. and Ozono, K. (2011). LEOPARD-type SHP2 mutant Gln510Glu attenuates cardiomyocyte differentiation and promotes cardiac hypertrophy via dysregulation of Akt/GSK-3beta/beta-catenin signaling. *Am. J. Physiol. Heart Circ. Physiol.* **301**, H1531-H1539.
Jopling, C., van Geemen, D. and den Hertog, J. (2007). Shp2 knockdown and Noonan/LEOPARD mutant Shp2-induced gastrulation defects. *PLoS Genet.* **3**, e225.
Keilhack, H., David, F. S., McGregor, M., Cantley, L. C. and Neel, B. G. (2005). Diverse biochemical properties of Shp2 mutants. Implications for disease phenotypes. *J. Biol. Chem.* **280**, 30984-30993.
Kim, J. H., Lee, S.-R., Li, L.-H., Park, H.-J., Park, J.-H., Lee, K. Y., Kim, M.-K., Shin, B. A. and Choi, S.-Y. (2011). High cleavage efficiency of a 2A peptide derived from porcine teschovirus-1 in human cell lines, zebrafish and mice. *PLoS ONE* **6**, e18556.
Kimmel, C. B., Ballard, W. W., Kimmel, S. R., Ullmann, B. and Schilling, T. F. (1995). Stages of embryonic development of the zebrafish. *Dev. Dyn.* **203**, 253-310.
Kontaridis, M. I., Swanson, K. D., David, F. S., Barford, D. and Neel, B. G. (2006). PTPN11 (Shp2) mutations in LEOPARD syndrome have dominant negative, not activating, effects. *J. Biol. Chem.* **281**, 6785-6792.
Krauss, S., Concordet, J.-P. and Ingham, P. W. (1993). A functionally conserved homolog of the Drosophila segment polarity gene hh is expressed in tissues with polarizing activity in zebrafish embryos. *Cell* **75**, 1431-1444.
Langdon, Y., Tandon, P., Paden, E., Duddy, J., Taylor, J. M. and Conlon, F. L. (2012). SHP-2 acts via ROCK to regulate the cardiac actin cytoskeleton. *Development* **139**, 948-957.
Legius, E., Schrander-Stumpel, C., Schollen, E., Pulles-Heintzberger, C., Gewillig, M. and Fryns, J.-P. (2002). PTPN11 mutations in LEOPARD syndrome. *J. Med. Genet.* **39**, 571-574.
Lien, C.-L., Harrison, M. R., Tuan, T.-L. and Starnes, V. A. (2012). Heart repair and regeneration: recent insights from zebrafish studies. *Wound Repair Regen.* **20**, 638-646.
Liu, D.-W., Hsu, C.-H., Tsai, S.-M., Hsiao, C.-D. and Wang, W.-P. (2011). A variant of fibroblast growth factor receptor 2 (Fgfr2) regulates left-right asymmetry in zebrafish. *PLoS ONE* **6**, e21793.
Long, S., Ahmad, N. and Rebagliati, M. (2003). The zebrafish nodal-related gene southpaw is required for visceral and diencephalic left-right asymmetry. *Development* **130**, 2303-2316.
Marin, T. M., Keith, K., Davies, B., Conner, D. A., Guha, P., Kalaitzidis, D., Wu, X., Lauriol, J., Wang, B., Bauer, M. et al. (2011). Rapamycin reverses hypertrophic cardiomyopathy in a mouse model of LEOPARD syndrome-associated PTPN11 mutation. *J. Clin. Invest.* **121**, 1026-1043.
Mendez, H. M. M. and Opitz, J. M. (1985). Noonan syndrome: a review. *Am. J. Med. Genet.* **21**, 493-506.
Mercola, M. and Levin, M. (2001). Left-right asymmetry determination in vertebrates. *Annu. Rev. Cell Dev. Biol.* **17**, 779-805.
Nakamura, T., Gulick, J., Pratt, R. and Robbins, J. (2009). Noonan syndrome is associated with enhanced pERK activity, the repression of which can prevent craniofacial malformations. *Proc. Natl. Acad. Sci. U.S.A.* **106**, 15436-15441.
Neel, B. G. and Tonks, N. K. (1997). Protein tyrosine phosphatases in signal transduction. *Curr. Opin. Cell Biol.* **9**, 193-204.
Neel, B. G., Gu, H. and Pao, L. (2003). The 'Shp'ing news: SH2 domain-containing tyrosine phosphatases in cell signaling. *Trends Biochem. Sci.* **28**, 284-293.
Neugebauer, J. M., Amack, J. D., Peterson, A. G., Bisgrove, B. W. and Yost, H. J. (2009). FGF signalling during embryo development regulates cilia length in diverse epithelia. *Nature* **458**, 651-654.
Nonaka, S., Tanaka, Y., Okada, Y., Takeda, S., Harada, A., Kanai, Y., Kido, M. and Hirokawa, N. (1998). Randomization of left-right asymmetry due to loss of nodal cilia generating leftward flow of extraembryonic fluid in mice lacking KIF3B motor protein. *Cell* **95**, 829-837.
Oishi, K., Gaengel, K., Krishnamoorthy, S., Kamiya, K., Kim, I.-K., Ying, H., Weber, U., Perkins, L. A., Tartaglia, M., Mlodzik, M. et al. (2006). Transgenic Drosophila models of Noonan syndrome causing PTPN11 gain-of-function mutations. *Hum. Mol. Genet.* **15**, 543-553.
Oishi, K., Zhang, H., Gault, W. J., Wang, C. J., Tan, C. C., Kim, I.-K., Ying, H., Rahman, T., Pica, N., Tartaglia, M. et al. (2009). Phosphatase-defective LEOPARD syndrome mutations in PTPN11 gene have gain-of-function effects during Drosophila development. *Hum. Mol. Genet.* **18**, 193-201.
Oteiza, P., Koppen, M., Concha, M. L. and Heisenberg, C.-P. (2008). Origin and shaping of the laterality organ in zebrafish. *Development* **135**, 2807-2813.
Oteiza, P., Koppen, M., Krieg, M., Pulgar, E., Farias, C., Melo, C., Preibisch, S., Muller, D., Tada, M., Hartel, S. et al. (2010). Planar cell polarity signalling regulates cell adhesion properties in progenitors of the zebrafish laterality organ. *Development* **137**, 3459-3468.
Qu, C. K. (2000). The SHP-2 tyrosine phosphatase: signaling mechanisms and biological functions. *Cell Res.* **10**, 279-288.
Ramsdell, A. F. (2005). Left-right asymmetry and congenital cardiac defects: getting to the heart of the matter in vertebrate left-right axis determination. *Dev. Biol.* **288**, 1-20.
Runtuwene, V., van Eekelen, M., Overvoorde, J., Rehmann, H., Yntema, H. G., Nillesen, W. M., van Haeringen, A., van der Burgt, I., Burgering, B. and den Hertog, J. (2011). Noonan syndrome gain-of-function mutations in NRAS cause zebrafish gastrulation defects. *Dis. Model. Mech.* **4**, 393-399.
Sarkozy, A., Digilio, M. C. and Dallapiccola, B. (2008). Leopard syndrome. *Orphanet J. Rare Dis.* **3**, 13.
Schramm, C., Fine, D. M., Edwards, M. A., Reeb, A. N. and Krenz, M. (2012). The PTPN11 loss-of-function mutation Q510E-Shp2 causes hypertrophic cardiomyopathy by dysregulating mTOR signaling. *Am. J. Physiol. Heart Circ. Physiol.* **302**, H231-H243.
Smith, K. A., Chocron, S., von der Hardt, S., de Pater, E., Soufan, A., Bussmann, J., Schulte-Merker, S., Hammerschmidt, M. and Bakkers, J. (2008). Rotation and asymmetric development of the zebrafish heart requires directed migration of cardiac progenitor cells. *Dev. Cell* **14**, 287-297.
Smith, K. A., Joziasse, I. C., Chocron, S., van Dinther, M., Guryev, V., Verhoeven, M. C., Rehmann, H., van der Smagt, J. J., Doevendans, P. A., Cuppen, E. et al. (2009). Dominant-negative ALK2 allele associates with congenital heart defects. *Circulation* **119**, 3062-3069.
Stewart, R. A., Sanda, T., Widlund, H. R., Zhu, S., Swanson, K. D., Hurley, A. D., Bentires-Alj, M., Fisher, D. E., Kontaridis, M. I., Look, A. T. et al. (2010). Phosphatase-dependent and -independent functions of Shp2 in neural crest cells underlie LEOPARD syndrome pathogenesis. *Dev. Cell* **18**, 750-762.
Tang, T. L., Freeman, R. M., Jr, O'Reilly, A. M., Neel, B. G. and Sokol, S. Y. (1995). The SH2-containing protein-tyrosine phosphatase SH-PTP2 is required upstream of MAP kinase for early Xenopus development. *Cell* **80**, 473-483.
Tartaglia, M., Mehler, E. L., Goldberg, R., Zampino, G., Brunner, H. G., Kremer, H., van der Burgt, I., Crosby, A. H., Ion, A., Jeffery, S. et al. (2001). Mutations in PTPN11, encoding the protein tyrosine phosphatase SHP-2, cause Noonan syndrome. *Nat. Genet.* **29**, 465-468.
Tessadori, F., van Weerd, J. H., Burkhard, S. B., Verkerk, A. O., de Pater, E., Boukens, B. J., Vink, A., Christoffels, V. M. and Bakkers, J. (2012). Identification and functional characterization of cardiac pacemaker cells in zebrafish. *PLoS ONE* **7**, e47644.
Thisse, C., Thisse, B., Schilling, T. F. and Postlethwait, J. H. (1993). Structure of the zebrafish snail1 gene and its expression in wild-type, spadetail and no tail mutant embryos. *Development* **119**, 1203-1215.
Tidyman, W. E. and Rauen, K. A. (2009). The RASopathies: developmental syndromes of Ras/MAPK pathway dysregulation. *Curr. Opin. Genet. Dev.* **19**, 230-236.
Van Vactor, D., O'Reilly, A. M. and Neel, B. G. (1998). Genetic analysis of protein tyrosine phosphatases. *Curr. Opin. Genet. Dev.* **8**, 112-126.
Yang, W., Klaman, L. D., Chen, B., Araki, T., Harada, H., Thomas, S. M., George, E. L. and Neel, B. G. (2006). An Shp2/SFK/Ras/Erk signaling pathway controls trophoblast stem cell survival. *Dev. Cell.* **10**, 317-327.
Yelon, D. (2001). Cardiac patterning and morphogenesis in zebrafish. *Dev. Dyn.* **222**, 552-563.
Yelon, D., Horne, S. A. and Stainier, D. Y. R. (1999). Restricted expression of cardiac myosin genes reveals regulated aspects of heart tube assembly in zebrafish. *Dev. Biol.* **214**, 23-37.
Yu, Z.-H., Xu, J., Walls, C. D., Chen, L., Zhang, S., Zhang, R., Wu, L., Wang, L., Liu, S. and Zhang, Z.-Y. (2013). Structural and mechanistic insights into LEOPARD syndrome-associated SHP2 mutations. *J. Biol. Chem.* **288**, 10472-10482.